Ultrasonics Sonochemistry 71 (2021) 105358

Contents lists available at ScienceDirect

Ultrasonics Sonochemistry

journal homepage: www.elsevier.com/locate/ultson

Ultrasonic effects on the headspace volatilome and protein isolate microstructure of duck liver, as well as their potential correlation mechanism

Le Xu [a], Qiang Xia [a,b,*], Jinxuan Cao [a,b,*], Jun He [a,b], Changyu Zhou [a,b], Yuxing Guo [c], Daodong Pan [a,b,d]

[a] Key Laboratory of Animal Protein Food Processing Technology of Zhejiang Province, College of Food and Pharmaceutical Science, Ningbo University, Ningbo 315211, China
[b] State Key Laboratory for Managing Biotic and Chemical Threats to the Quality and Safety of Agro-products, Ningbo University, Ningbo 315211, China
[c] Department of Food Science and Technology, School of Food Science and Pharmaceutical Engineering, Nanjing Normal University, Nanjing 210023, China
[d] National R&D Center for Freshwater Fish Processing, Jiangxi Normal University, Nanchang, Jiangxi 330022, China

ARTICLE INFO

Keywords:
Ultrasonic effects
Off-flavor
Volatile fingerprint
Duck liver protein isolate
Molten-globule state

ABSTRACT

In spite of the high added value and tremendous output from duck processing industries, duck liver (DLv) is underutilized and a major factor is related to its prominent off-flavor perception which hampers the consumption and processing attributes. This work was designed to investigate the impact of low-frequency ultrasound (US) pretreatments on the headspace volatilome evolution of DLv and its isolated protein (DLvP) microstructure, aiming at exploring the potential of US technology to inhibit off-flavor perception and possible mechanisms behind. Results suggested that US pretreatment resulted in decreased lipid oxidation and off-flavor perception, simultaneously without significantly causing physicochemical influence including texture, pH and color. US induced obvious tertiary structural changes of DLvP, as revealed by the intrinsic fluorescence and surface hydrophobicity (H0), whereas the SH, S-S, secondary structure and molecular weight of DLvP remained unaffected, suggesting the presence of molten globule state (MG-state) under ultrasonic conditions. Besides, the headspace contents of flavor compounds, mainly aldehydes and alcohols, were significantly decreased whereas acids were increased. Multivariate analysis suggested an obvious US-induced effect on the volatilome evolution of DLv samples. Discriminant analysis recognized the aroma compounds including aldehydes and alkenals as the major contributors leading to the change of olfactory characteristics of DLv after ultrasonic treatment. Correlation analysis demonstrated the positive relationship between the volatile markers variation and the increased H0 values, a characteristic attribute of MG-state protein. The results obtained in this work suggested that US technology matched with suitable parameters could be a very promising approach to modulate the off-flavor perception of liver products by altering DLvP conformation.

1. Introduction

As a major by-product from duck processing, duck liver (DLv) is generally rich in proteins, vitamins and minerals, of which the production increases rapidly with the introduction of automatic segmentation beltline. Apart from a very minimal proportion of DLv used for direct consumption and supplementary materials for processed foods, most of the liver produced during industrial manufacturing of duck meat is processed into fertilizer or feeding stuff. One of major reasons explaining the limited consumption of liver is related to its prominent off-flavor perception which may arise from the animal feeding and intrinsic metabolism [1]. The objectionable odor could be described as intensely fishy or metallic, as characterized by Strasser and Schieberle [2]. Although great efforts aiming at reducing the perception of DLv off-flavor, such as masking off-flavor regents, physical deodorization, and modification of food matrix have been made, related techniques require further optimization and development for mitigating liver off-flavor in an economical, efficient and environmentally friendly way.

* Corresponding authors at: Key Laboratory of Animal Protein Food Processing Technology of Zhejiang Province, College of Food and Pharmaceutical Science, Ningbo University, Ningbo 315211, China.
E-mail addresses: xiaqiang@nbu.edu.cn, xqiang0713@hotmail.com (Q. Xia), caojinxuan@nbu.edu.cn (J. Cao).

https://doi.org/10.1016/j.ultsonch.2020.105358
Received 21 July 2020; Received in revised form 27 September 2020; Accepted 1 October 2020
Available online 7 October 2020

The olfactory property of food products is one of the most important quality parameters determining consumer preference, closely associated with the headspace concentration of flavor compounds. As a high-bioavailability food matrix, animal-derived proteins are known to combine with a variety of flavor compounds by reversible and irreversible binding, thus influencing the retention and release process of volatile flavor compounds such as aldehydes, alcohols, ketones, esters and pyrazines. For example, Herrera-Jimenez, Escalona-Buendia, Ponce-Alquicira, Verde-Calvo and Guerrero-Legarreta [3] have concluded that the detected concentrations of pyrazines were decreased significantly due to hydrophobic interactions between myofibrillar protein and ethyl/methyl pyrazines radicals. In addition, irreversible covalent bond can also play an important role in protein-flavor interaction, as demonstrated in the case of the binding of aldehydes to soy protein by Kuehn, Considine and Singh [4] and Suppavorasatit and Cadwallader [5]. However, the affinity of binding between flavor compounds and protein acts as a multi-factors function, including protein conformation, composition, and the physicochemical attributes of flavor compounds [6]. Wang, Zhao, Qiu and Sun [7] reported that the binding of native soy protein isolate with flavor compounds decreased in the order *trans*-2-nonenal > nonanal > *trans*-2-octenal > *trans*-2-hexenal > hexanal > 1-octen-3-ol, proving that the binding between flavor compound and protein is affected by the type and structure of flavor compounds. More recently, Guo, He, Wu, Zeng and Chen [8] reported that the changes of protein conformation induced by high molar binding ratio of flavor results in non-linear binding between protein and flavor compounds. Overall, the enhancement of binding affinity between protein and flavor compounds can reduce the impact of undesirable flavors by inhibiting the release process and headspace concentrations of off-flavor components during food processing and preservation.

As a novel technology to modify protein structure and properties, ultrasound (US) has recently been received increasing attention for mining its innovative applications [9,10]. Particularly, in protein-rich food, US is employed as a non-thermal processing approach for maximally maintaining the sensory attributes of the product, and final influence is related with cavitation, shear stresses, dynamic agitation and turbulence. It is generally recognized that US-mediated modification in the functional properties of protein isolate is achieved by ultrasound driven conformational changes of treated protein, depending on process parameters, protein sources and processing patterns [11–13]. Recently, several articles have reported the volatilome evolution of different food systems responding to US pretreatments, but the variations in volatile fingerprinting were mainly discussed and explained in terms of US-induced chemical reactions, including Maillard reaction, Strecker degradation or lipid oxidation [14]. To the best of our knowledge, few literatures have investigated the contribution of US-induced structural changes of protein to the volatilome evolution. Therefore, there is very limited information concerning structure–function relationship for the protein-flavor binding behavior under US conditions, which is necessary for flavor quality control and explaining the headspace concentration changes of US-processed foods.

The objective of this study was to investigate the effects of low-frequency US pretreatments on the physicochemical and sensory attributes as well as the volatile fingerprinting of DLv, aimed at exploring the potential of US technology to mitigate off-flavor in liver products for the use in the food industry. The physicochemical attributes of DLv include thiobarbituric acid reactive substances (TBARS), chromatic aberration, pH and texture. In addition, the structural properties of DLvP were analyzed, including SH, S-S, surface hydrophobicity, intrinsic fluorescence, and SDS-PAGE, to reveal the potential correlation with the volatilome evolution induced by ultrasonic effects.

2. Materials and methods

2.1. Materials and sample preparation

Three types of fresh DLv, produced from different duck varieties with about 45 days of age, labeled as DlAck, DlBck and DlCys respectively, were purchased from a local commercial abattoir (Ningbo, China). The samples were separated from the large blood vessels and bile ducts, packed and frozen at −40℃, and used within 15 days. Before the experiment, the packed samples were stored overnight in a refrigerator at 4℃. The livers were transferred to a cup and mashed by blender (MX-GX1011, Panasonic, Japan). Three types of mash liver were divided into two groups evenly and then packed in polyethylene bag respectively. The experimental group was treated with KS-300 EII ultrasonic equipment (Kesheng Co., Ningbo, China) for 30 min at 40 kHz and 600 W (US), and the other group was used as control group (NUS). Samples were taken randomly for analysis, and assays were done in triplicate. All the reagents and chemicals used were of analytical grade.

DLvP was prepared according to Wang and Arntfield [15] and Xiong, Gao, Wang, Xu and Zhou [16] with few modifications. A total 10.00 g of minced DLv was accurately weighed and then homogenized in ice bath with 50 mL of pre-cooled 0.6 M NaCl (20 mM phosphate, pH 7.0) solution in a break using a high-speed homogenizer (Scientz Co., Ningbo, China) at 12000 rpm for 3 × 15 s. After standing for half an hour, the homogenate was centrifuged with a refrigerated centrifuge (Hunan Xiangyi, Laboratory Instrument Development Co., Changsha, China) at 8000 × g and 4℃ for 10 min. Then, ammonium sulfate was added to the separated supernatant until the solution reaches 60% saturation, and standing overnight in a refrigerator at 4℃. The protein suspension was centrifuged using a refrigerated centrifuge at 12000 × g and 4℃ for 20 min. The lower sediment was collected and placed in a dialysis bag with 8000–14000 D (Beijing Solarbio Science & Technology Co., Beijing, China) which was soaked in 20 mM phosphate buffer (pH 7.0) at 4℃. The phosphate buffer shall be changed every 6 h until the dialysate meets $BaCl_2$ reagent without white precipitate. The dialysate was then freeze dried with a vacuum freeze dryer (ALPHA 1–4 LD plus; Martin Christ, Osterode, Germany), and the dry powders were stored at −40℃ for further treatment.

2.2. Ultrasound treatment of protein solutions

The concentration of DLv protein was adjusted with distilled water, and divided into two parts (NUS and US). The US group was treated under ultrasound equipment at 40 kHz for 30 min and NUS was used as control group. Samples were taken randomly for sodium dodecyl sulfate–polyacrylamide gel electrophoresis (SDS-PAGE), S-S, SH group, surface hydrophobicity, intrinsic fluorescence, scanning electron microscopy and circular dichroism analysis.

2.3. Measurement of lipid oxidation

TBARS value was measured according to Zhang et al. [17] with few modifications. Two-gram portions of DLv were homogenized with 10 mL of 20% trichloroacetic acid (containing 0.1% EDTA) at 3000 rpm for 3 × 10 s while cooled on ice using a DY89-I high-speed homogenizer. The homogenate was then filtered through Whatman No.1 filter paper. Each of filtrate was added 1 mL of 0.02 M 2-thiobarbituric acid, shaken for 1 min, heated by a metal bath at 100℃ for 40 min and cooled to room temperature. The solution was centrifuged at 1600 × g and 4℃ for 10 min. 1 mL supernatant was added with 1 mL trichloromethane, shaken for 1 min, against a blank prepared same as the experience group without sample. The absorbance of the resulting solution was measured at 600 nm and 532 nm by a Reader M200 (Tecan, Austria). Assays were done in triplicate. The TBARS value was calculated by the following equation: TBARS (mg kg^{-1}) = (A532 − A600) / 155 × 0.5 × 72.6 × 1000.

2.4. Determination of pH

Five-gram portions of DLv were placed in a 50-mL test tube and homogenized at 3000 rpm for 3 × 10 s with 20 mL distilled water using a homogenizer, and then homogenate solutions were used for pH determination with a pH meter (Five Easy Plus FE28, Mettler Toledo, China).

2.5. Determination of chromatic aberration

Lightness (L*), redness (a*), and yellowness (b*) were determined following the recommendations of Zhang et al. [17] using a chromatic meter (CR- 400 Konica Minolta Investment Ltd, Tokyo, Japan). The L*, a*, and b* value corresponded to lightness, redness, and yellowness, respectively. Color measurements were carried out at room temperature in triplicate.

2.6. Determination of texture profile

The textural analyses were performed using a TA-XT Plus Texture Analyser (Stable Micro System, Surrey, UK) equipped with a load cell of 1 kg and a 35 mm extrusion probe (A/BE35). 20 g of minced sample was added to sample container. Texture profile analyses (TPA) method was used to evaluate the texture based on the compression of the sample. The pre-test speeds, test speeds and post-test speeds were 0.5 mm/s, 0.3 mm/s and 1 mm/s, respectively, and target value was set as 5 mm. Texture profile parameters were computed, namely adhesiveness, cohesiveness, resilience. Assays were done in triplicate.

2.7. Sensory characterization

Sensory evaluation and E-nose analysis were performed to characterize the effects of US treatment on the off-flavor perception. Three types duck livers were minced and then treated with and without US treatment. 5 g of samples was taken into the headspace extraction vial and sealed, balanced in a water bath at 30℃ for 30 min for sensory evaluation and an E-nose. The team of sensory evaluation consists of 10 trained panelists with ages of 22–28. They were asked to sniff the headspace above the samples after opening the cover and score the samples using a 10-point scale, where 0 represented no off-flavor and 10 represented the strongest off-flavor. The electronic nose (PEN3 system, Airsense Analytic Co. Ltd., Schwerin, Germany) was used in electronic nose analysis, equipped with 10 metal oxide semiconductor (MOS) type chemical sensors, including W1C (aromatic), W5S (broad range), W3C (aromatic), W6S (hydrogen), W5C (aromatic aliphatics), W1S (broad methane), W1W (sulfur organic), W2S (broad alcohol), W2W (sulfur chlorine) and W3S (methane aliphatics). Detection parameters were listed as follows: the sampling interval: 1 s; flush time: 100 s; the sensor zero time: 10 s; the pre-sampling time: 5 s; the injection flow rate: 150 mL min^{-1} and 300 s for sampling analysis. The data acquisition system collected the signals which were processed further at 150 s for data analysis.

2.8. Determination of volatile compounds

Volatile compounds were characterized in accordance with our recent literature [18]. Grounded samples (4.0 g) and NaCl (0.1 g) were added into headspace sample vial, sealed and equilibrated at 4℃ for 16 h. Volatile compounds were extracted using a 75 μm carboxen/polydimethylsiloxane fiber at 45℃ for 30 min. The volatile compounds adsorbed by the fiber were separated on a VLCOL capillary column (60 m × 0.32 mm × 1.8 μm film thickness), identified and quantified by mass-selective detector. Helium was used as the carrier gas. The oven was held at 35℃ for 3 min, heated to 40℃ at 3℃ min^{-1}, maintained for 1 min, ramped to 210℃ at 5℃ min^{-1} and finally held for 11 min. Mass spectrum was obtained in EI mode (0.9 kV) and scanned at the range of *m/z* 45–600. Detector temperature was set at 200℃. Volatile compound was identified based on retention time and the mass spectra in NIST14 databases. Assays were done in triplicate.

2.9. Determination of the surface hydrophobicity (H0)

The H0 was determined using 1-anilino-8-napthalenesulfonate (ANS) and described by Lou, Yang, Sun, Pan and Cao [19]. The 10 μL aliquot of 8 mmol L^{-1} ANS (0.1 mol L^{-1} KH_2PO_4 buffer, pH 7.0) was added to 2 mL of protein solution under agitation for 1 min. The control consisted of 10 μL of 8 mmol L^{-1} ANS (0.1 mol L^{-1} KH_2PO_4 buffer, pH 7.0) and 2 mL of 15 mM Tris-HCl buffer (pH 7.0). Samples and controls were kept under dark condition, and incubated at 37 °C for 10 min. Fluorescence intensity of the solutions was measured using a M200 Reader (Tecan, Austria) at excitation and emission wavelengths of 370 and 480 nm, respectively. The initial slope of the plot of fluorescence intensity versus protein concentration was calculated to obtain the H0 values. The assays were performed in triplicate.

2.10. Determination of SH and S-S group levels

The concentration of DLvP solution was adjusted to 1 mg mL^{-1} with 30 mM Tris-HCl buffer. The SH and S-S group levels were determined according to the method described by Du et al. [20]. To determine SH group level, 0.5 mL DLvP solution was incubated with 2.5 mL Tris-Gly-8 M Urea and 20 μL of 4 mg mL^{-1} 5,5-dithiobis-2,2-nitrobenzoic acid (DTNB) for 30 min at 25°C. The SH group level was expressed as follows:

SH group level (μmol g^{-1} liver protein) = 73.53 A_{412} D/C

Where D is the dilution coefficient (6.04); C (mg ml^{-1}) is the protein concentration.

For determining the S-S group level, 0.2 mL of DLvP solution was incubated with 1.0 mL Tris-Gly-10 M Urea and 0.02 mL of 2-mercaptoethanol for 1 h (25°C). After mixing with 10 mL of 12% (w/v) trichloroacetic acid and stranding for 1 h, the sample was subjected to centrifugation at 3000 × g for 10 min. Then the residues were dissolved in 3 mL of Tris-Gly-8 M urea and 0.03 mL of DTNB (4 mg mL^{-1}). The absorbance of samples was measured at 412 nm after incubation at 25℃ for 30 min. The S-S group level was expressed as follows:

S-S group level (μmol g^{-1} liver protein) = 73.53 A_{412} D/C – SH group level

Where D is equals to 15.

2.11. Determination of intrinsic fluorescence

The intrinsic emission fluorescence spectra of the protein samples were obtained by a M200 Reader according to Liu et al. [21]. The concentration of DLvP solution was adjusted to 1 mg mL^{-1} with 10 mM phosphate buffer (pH 6.2). To minimize the contribution of tyrosine residues to the emission spectra, the protein solutions were excited at 290 nm, and the emission spectra were recorded from 285 to 315 nm at a constant slit of 2 nm for both excitation and emission. All the measurements were conducted in triplicate.

2.12. Scanning electron microscopy (SEM)

The morphology of the lyophilized DLvP sample was observed with a scanning electron microscope (S-3400 N, Japan) at accelerating voltage of 10 Kv. Before SEM characterization, the samples were sputtered with gold using an ion sputter coater (E-1010, Hitachi high-tech science systems co., Japan) for 120 s. The SEM photographs were obtained at 2.5 K magnification.

2.13. Circular dichroism (CD)

CD spectra were scanned at the far-UV range from 190 to 260 nm in 0.1 cm quarz cuvette (Hellma, Muellheim, Baden, Germany) with a CD spectropolalarimeter (J-1500, Jasco Co., Japan). The concentration of

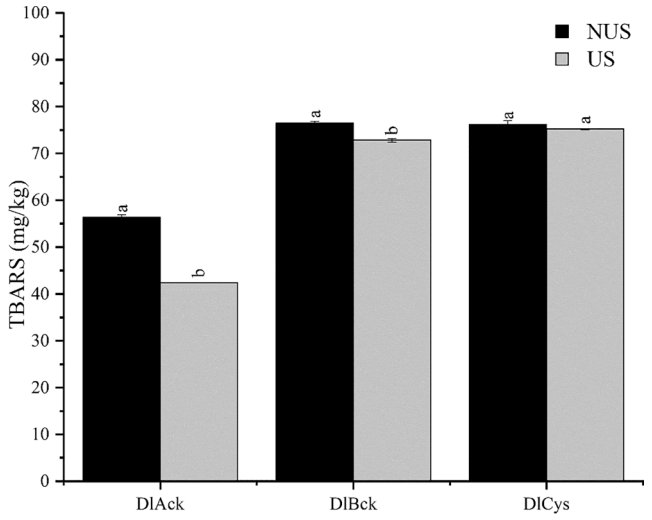

Fig. 1. Effects of ultrasound pretreatment on TBARS in three types DLv. The data are expressed as the mean of three measurements; and error bars show the standard deviations; different letters between NUS and US indicate statistically significant differences at $p < 0.05$.

DLvP for CD analysis was 0.5 mg ml^{-1}. The values of scan rate, response, and band width were 50 nm min^{-1}, 0.25 s and 1.0 nm, respectively. Three scans were averaged to obtain one spectrum. Secondary structures were calculated according to Yang's reference software, provided by Jasco Corp, including α-helix, β-sheet, β-turn and random coil.

2.14. SDS-PAGE

SDS-PAGE was performed by SDS-PAGE Preparation kit (Sanggon Biotec Co., Shanghai, China). 3 mg ml^{-1} DLvP were dissolved in the sample loading buffer, and then heated at 100℃ for 10 min. Samples were separated on 12% resolving gel and 5% stacking gel. Ten microliters of each sample were loaded onto the gel and subjected to electrophoresis at voltage of 80 V in stacking gel and 120 V in resolving gel using a DYCZ-24DN Electrophoresis Cell (Beijing LiuYi Biotechnology CO., LTD). Low molecular weight markers (11–245 kDa) were run as a reference.

2.15. Statistical analysis

Statistical analysis was performed with the SPSS 19.0 software (IBM CO., USA). Independent-samples T tests were carried out to analyze the significant differences of SH, S-S, surface hydrophobicity, TBARS, color parameters (L*, a*, and b*), textural attributes, pH and CD. Difference between the means of treatments was considered significant at $p < 0.05$. The results were expressed as mean value ± standard deviation. Chromatographical data were processed using GC–MS Solution Workstation software Ver. 4 (Shimadzu, Kyoto, Japan) and expressed as the peak area each compound which was visualized by processed chromatographical data by importing into MultiExperiment Viewer (MeV) software (ver. 4.9; DanaFarber Cancer Institute, Boston, MA, USA). After normalization (Pareto scaling), in order to evaluate the ultrasound effects on the volatile shifts, a supervised model, orthogonal projections to latent structure-discriminant analysis (OPLS-DA), was established using SIMCA-P software (ver. 14.1, UMETRICS, Umea, Sweden). The presence of outliers was examined by Hotelling's T2 with 95% confidence. In addition to the calculation of R2 and Q2 metrics, the analysis of variance testing of cross-validated predictive residuals (CV-ANOVA, p-value < 0.05) and permutation testing (n = 200) were also used to evaluate the robustness of the established OPLS-DA model.

3. Results and discussion

3.1. Physicochemical changes in DLv after US pretreatment

Physicochemical analysis was performed to assess the effect of US pretreatment on the quality attributes of DLv, suggesting that US treatments had no significant influence on physicochemical parameters including color, textural properties and pH (Table S1). Similar changes after exposure to US treatments of muscle systems have been reported, as in the cases of the pH in pre-rigor muscle [22], of the adhesiveness and resilience of beef semitendinosus muscle [23], and of all the color parameters (L*, a*, and b*) of bovine Semitendinosus and Longissimus muscles [23,24]. In this work, limited US-induced effects on physicochemical parameters were related to the minced forms of DLv samples and the short time after ultrasonic treatment. For example, there were no significant changes in textural feature immediately after sonication, but greatly improved ($p < 0.05$) firmness was observed for the stored samples with US treatment [25].

In contrast, TBARS, as an index for the evaluation of degree of unsaturated fatty acid oxidation, were significantly decreased ($p < 0.05$) after ultrasonic treatment in Fig. 1, indicating that mild US pretreatment may inhibit the formation of lipid oxidation of DLv. For DLv, it can be consumed as a supplementary source for long-chain omega-3 fatty acids, due to the high conversion efficiency of dietary fat in duck [26]. Simultaneously, a high capacity of lipogenesis results in the high lipid content of DLv. Thus, the lipid stability during processing is of great importance for maintaining the flavor quality of DLv-based products.

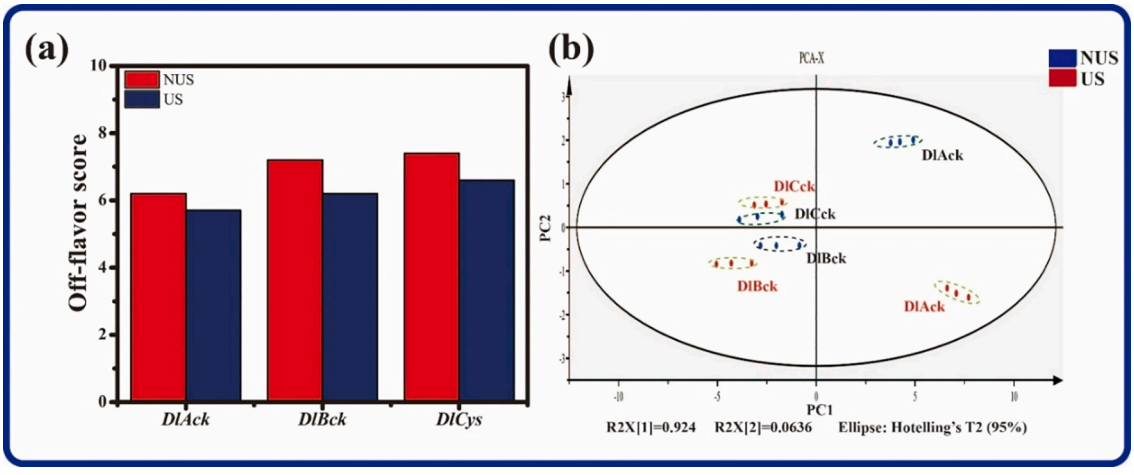

Fig. 2. Effects of US pretreatment on the off-flavor perception of DLv according to sensory (a) and E-nose analysis (b).

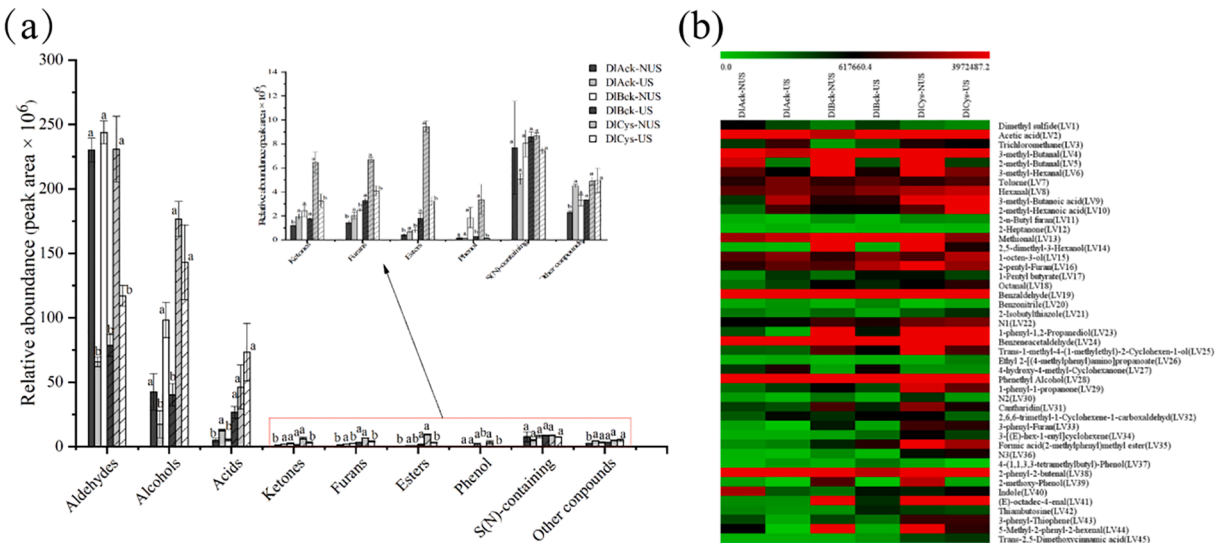

Fig. 3. (a) Changes in the abundance of volatile components grouped in chemical classes between NUS and NS in three types of DLv. a, b different letters between NUS and US for same DLv types indicate statistically significant differences at $p < 0.05$; (b) Heatmap visualization of volatile organic compounds of NUS and US in three types of DLv.

Regarding the decrease in TBARS contents after US, it could be attributed to the influence of US treatment on the protein structure and the exposure of reducing amino acid residues to the surface of DLv protein, similar to the delayed effects of US-treated whey protein on the lipid oxidation of salmon pieces [27]. Simultaneously, it was noted that US can also result in different patterns of the response of the lipid oxidation

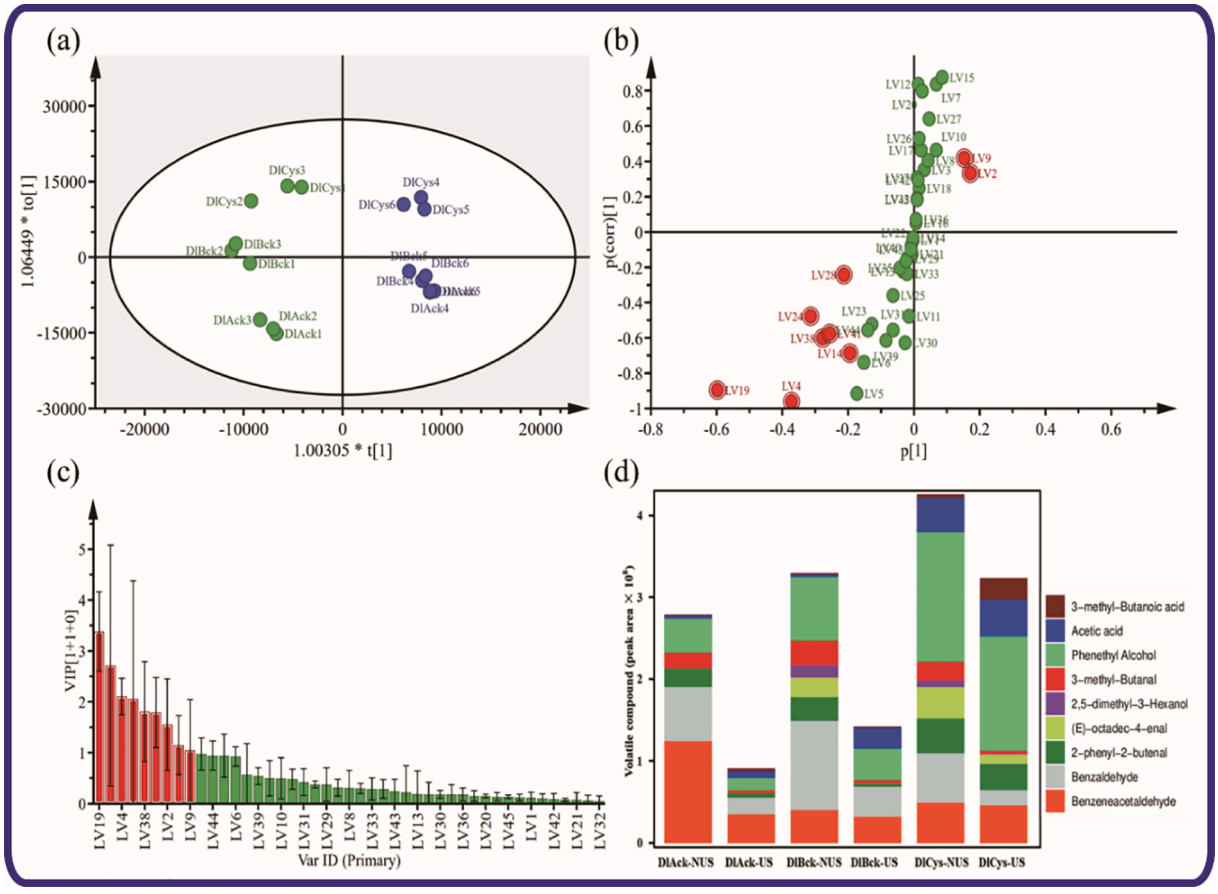

Fig. 4. The scores plot (a), loading S-Plot (b), a VIP plot (c) and relative abundance of potential marks (d) of OPLS-DA model (R2X = 0.71, R2Y = 0.957, Q2 = 0.936, CV-ANOVA *p*-value 1.25×10^{-7}), generated by the comparison between the NUS and US, to discriminate US-treated samples from the untreated samples in three types of DLv. The S-plot shows that the covariance p [1] against the correlation p(corr) [1] of the variables of the discriminating components of the OPLS-DA model; the chosen variables are highlighted in the S-plot (|p [1]|>0.1; |p(corr) [1]|>0.2; VIP > 1). VIP > 1 was marked as red in (c). (For interpretation of the references to color in this figure legend, the reader is referred to the web version of this article.)

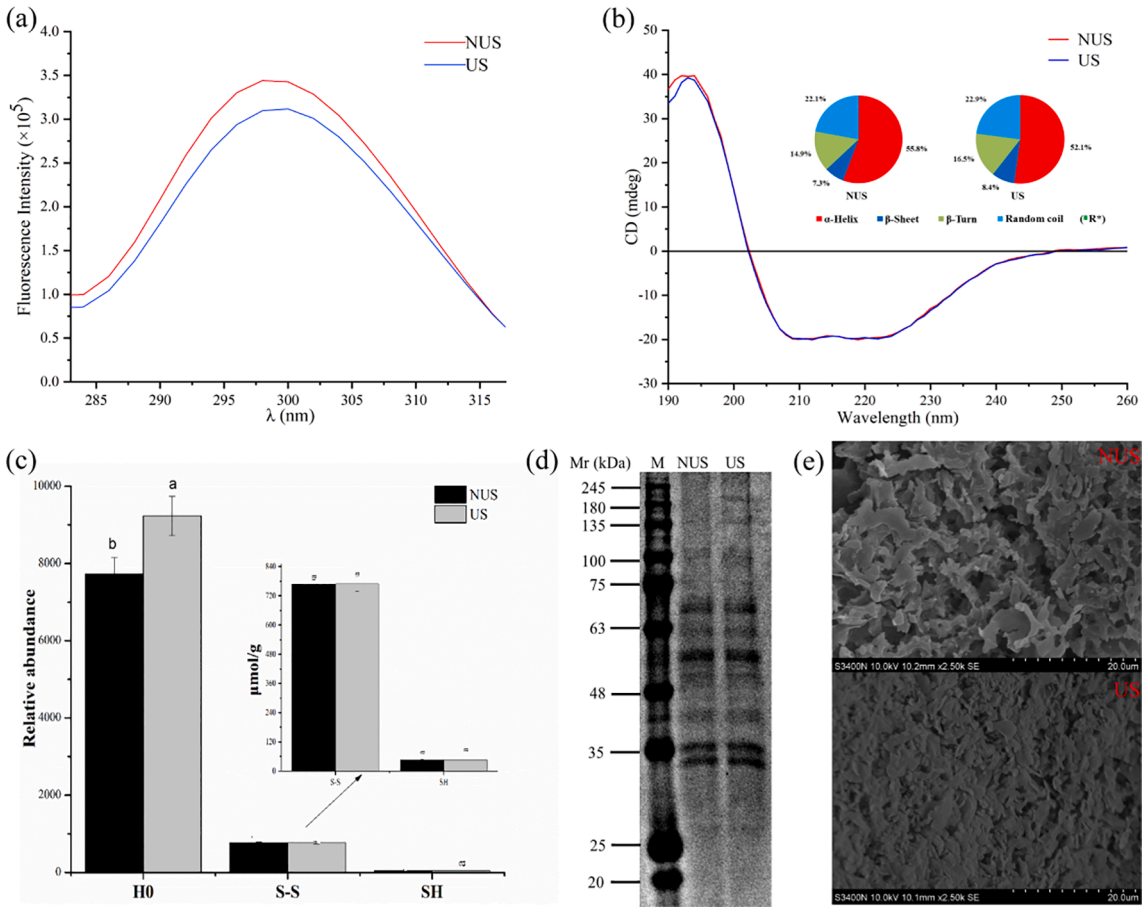

Fig. 5. (a) Intrinsic fluorescence intensity; (b) Far-UV circular dichroism (CD) spectra (* letter indicate statistically significant differences at $p < 0.05$, n = 3); (c) Effects of ultrasound on the surface hydrophobicity (H0), SH, and S-S of DLvP. Different letters indicate statistically significant differences at $p < 0.05$, n = 3; (d) SDS-PAGE profiles (M, molecular weight marker, NUS, Lane 1; US, Lane 2); (e) Scanning electron microscopy microscope of NUS and US. Scale bars indicate 20 μm.

degree to US treatments, as exemplified by the improved TBARS in spiced beef [28], suggesting that the US effects on lipid oxidation are dependent on food matrices and processing parameters. Overall, these results demonstrated that US pretreatment shows no negative influence on the physicochemical attributes of the final products and even favors the quality stability.

3.2. Ultrasonic effects on off-flavor perception

According to Fig. 2a, US treatment resulted in the decrease of the off-flavor perception of all types of DLv samples. E-nose has been proved to be robust for processing methods evaluation and analysis of product aroma differentiation, due to its speed, simplicity, and high sensitivity [29]. To confirm the results of sensory evaluation, the instrumental analysis (E-nose) was performed and the PCA results based on E-nose information are shown in Fig. 2b, demonstrating a clearly differentiated olfactory pattern between the US-treated and untreated DLv samples. The first two interpretable factors (PC1 and PC2) explained 98.8% of the total variance. PC1, with 92.4% of the variance explained, mainly discriminated the different DLv samples. Although PC2 gives relatively lower data interpretation rate than PC1, it can completely discriminate aroma notes of the DLv samples with and without US treatment. The untreated DlAck is distributed at the positive axis of PC2 while the treated samples are distributed at the negative axis (Fig. 2b). It was also noted that although the points of other samples, including DlBck and DlCck, present near distribution, the ultrasonicated and unultrasonicated samples are separated from each other according to PC2. These results have indicated that US treatment exerts a clear influence on the sensory perception of flavor features of DLv samples. Nevertheless, the specific mechanisms governing the ultrasonic effects on flavor perception require further investigation.

3.3. Analysis of the headspace volatilome of US-pretreated DLv

To characterize the effects of US treatments on aroma fingerprinting, HS-SPME coupled to GC–MS was used to extract and detect the aroma compounds of all the DLv samples. A total of 45 volatile compounds in three kinds of DLv were identified by SPME-GC–MS, and classified into nine different chemical groups (Table S2), including aldehydes (11), alcohols (5), acids (4), ketones (4), esters (2), S(N)-containing compounds (10), furans(3), phenol (2) and other compounds (4). According to Fig. 3a, aldehyde displays the highest number of compounds in the livers examined, in consistent with the findings observed in other types of liver [30]. Furthermore, it was also observed that the content of aldehydes in all DLv decreased significantly ($p < 0.05$) after ultrasound treatment, and similar changing pattern was found for alcohols. Comparatively, the content of acids showed an increasing trend, and S (N)-containing did not change significantly ($p > 0.05$). Similar results have been obtained by Perez-Santaescolastica et al. [31], reporting that ultrasonic treatment was able to reduce the content of aldehydes in dry-cured ham.

Overall, aldehydes, with characteristic aroma notes such as butter, sweet, floral, toasted or green odors, have low odor thresholds and are present in higher amounts thus playing an important role to the flavor of food products. Among all aldehyde identified in DLv (Fig. 3b), 3-methyl-butanal, 3-methyl-hexanal, hexanal, benzaldehyde, 2-pheny-2-buteanl

and benzeneacetaldehyde are the major compounds, quantitatively. According to previous literatures, the linear hexanal is derived from ω-6 unsaturated fatty, with intense grass-like notes, and is determined to exist in large quantities in Nanjing marinated duck [32]. As for 3-methyl butanal, benzeneacetldehyde, benzadehyde and 2-pheny-2-buteanal, described with nutty, acorn, bitter almond and sweet respectively, significantly contribute to the overall flavor of meat product [14,33–35]. Except for the aldehydes mentioned above, methional, 1-octen-3-ol, 2-pheny-furan, phenthyl alcohol and acetic acid also were founded in DLv in large quantities, described by mashed potato, vegetable, mushroom, rose and vinegar notes, respectively [36,37]. In term of the specific olfactory characteristics of volatile compounds, the above-mentioned volatile organic compounds, especially aldehydes, may contribute to the perception of off-flavor of DLv when their concentrations exceed certain ranges [38].

In order to reveal the volatile fingerprinting pattern shifts and identify potential volatile markers among different DLv samples responding to US treatment, the OPLS-DA model was then generated as represented in Fig. 4. As a supervised binary classification approach, the presence of over-fitting problems of this model could be excluded based on the quality parameter ($Q^2 = 0.936$) and a permutation testing with 200 iterations. Simultaneously, a clear separation with a high-fitting quality ($R^2X = 0.741$, $R^2Y = 0.957$) was observed in the OPLS-DA score plot (Fig. 4a). There are no marked overlapping of NUS and US and can be drawn as two relatively independent discrete entities, and then confirmed by hierarchical clustering analysis (Figure S1). Furthermore, coupled with the OPLS-DA loading S-plot (Fig. 4b), nine discriminating volatile compounds, including benzaldehyde, phenethyl alcohol, 3-methyl-butanal, benzeneacetaldehyde, (E)-octadec-4-enal, 2-phenyl-2-butenal, acetic acid, 2,5-dimethyl-3-hexanol and 3-methyl-butanoic acid could be selected to explain the observed differential sample clustering. To avoid variable selection bias [39], the significance of the variables from the loading S-plot was assessed using, firstly, the variable importance in projection (VIP) plot (Fig. 4c). According to Fig. 4d, the variation between NUS and US could be mainly responsible for the changes of aldehydes, alcohols and acids. In terms of individual compounds (Fig. 3b), US decreased the contents of most of US-associated marker volatile compounds in DLv, especially benzaldehyde, 3-methyl-butanal, benzeneacetaldehyde, (E)-octadec-4-enal, 2-phenyl-2-butenal, 2,5-dimethyl-3-hexanol, phenethyl alcohol, whereas acetic acid and 3-methyl-butanoic acid increased. The unsaturated aldehydes and ketones were identified as the major off-flavor compounds of liver products [40]. Thus, the decreased aldehydes, particularly alkenals, could be the major reason responsible for explaining the decrease in the off-flavor perception in terms of volatile fingerprinting. Simultaneously, the increased headspace acid components had a sheltering effect on the perception of DLv off-flavor as a result of the odor balance. Regarding the response of headspace concentration to immediate US treatment, the interactions between DLv protein and related volatile flavor should be analyzed from all perspectives, particularly the ultrasonic influence on protein structure.

3.4. Analysis of structural modification of DLvP after US pretreatment

3.4.1. Surface hydrophobicity

Protein surface hydrophobicity depends on exposed amino acid residues to polar aqueous environment and can be used to measure changes in the spatial structure of proteins. The surface hydrophobicity exhibited by fluorescence emission spectra of NUS and US are shown in Fig. 5c. Compared with NUS, the surface hydrophobicity of US increased significantly, in consistent with the previous research results [41,42]. It indicated that ultrasonic treatment can induce protein unfolding and expose hydrophobic residues hidden within protein molecules to protein surface.

3.4.2. Levels of S-S and SH groups

As shown in Fig. 5c, the SH and S-S group levels of NUS were 46.02 and 768 μmol g^{-1} respectively, but neither SH nor S-S were remarkably changed as a result of ultrasound treatment ($p > 0.05$). Previous results suggested that US can modify the SH and S-S contents of protein isolate [43,44]. This difference might arise from the differences in the intensity and duration of the applied ultrasound. Another possibility is that the intra-molecular location of the SH and S-S in DLvP examined here may also make them less susceptible to degradation by ultrasound.

3.4.3. Intrinsic fluorescence emission spectroscopy

Fluorescence spectroscopy is a useful technique to investigate tertiary structure transition in proteins because the intrinsic fluorescence of aromatic amino acid residues is sensitive to the polarity of microenvironments along the transition. When a protein unfolds, the chromophores become exposed to solvent, resulting in the decreased fluorescence intensity [45]. Intrinsic fluorescence emission spectra of NUS and US are presented in Fig. 5a. A maximum of fluorescence emission was found at 298 nm, and the wavelength of fluorescence emission peak was not shifted. However, US treatment resulted in decrease in the intensity of the fluorescence. Similar results have also been obtained by Zhang et al. [11]. A reasonable explanation for this is that the tertiary structure of the protein has been changed by the cavitation effect of ultrasound, causing more chromophores to be exposed to the solvent and decreasing the fluorescence intensity.

3.4.4. SDS-Page

SDS-PAGE profiles of the samples are shown in Fig. 5d. Comparison with the NUS group shows that ultrasonic treatment did not induce major changes in the protein electrophoresis profiles, indicating that ultrasonic treatment presented no obvious effects on primary structure of the DLv proteins. Similar results have also been obtained in the SDS-PAGE studies of soybean protein isolate and peanut-protein, in which all bands were intact and no extra fragments or dimerization were observed [11,43].

3.4.5. SEM

The microstructures of NUS and US-treated DLvP are presented in Fig. 5e. Compared to the loose structure of NUS, the structure of US became dense and accompanied by decrease the micropores. Meanwhile, the large size of protein can be seen in untreated DLvP, composed of discrete entities, whereas US-pretreated DLvP shows an obvious aggregation phenomenon. These microstructural changes may be due to the oscillating waves generated and local micro-jets by ultrasonic cavitation leading to the increased surface hydrophobicity of protein and resultant reorganization by aggregation [46]. For example, the exposure of the aromatic amino acid residues to solvent contributes to increase surface hydrophobicity and fluorescence quenching. The microstructural modification was driven by the damage of hydrogen bonds and van der Waals forces between protein molecules under US conditions [46–47]. Moreover, the decreased TBARS values may be related to the altered protein microstructure which led to the exposure of reducing amino acid residues, such as cysteine, of which the oxidization into disulfide bonds promoted the aggregation of proteins and the bury in the intra-aggregates.

3.4.6. CD

Circular dichroism can reflect the changes of the protein backbone peptide bond conformation, and the percentage of secondary structure between NUS and US is shown in Fig. 5b. The estimated secondary structure of NUS was 55.8% for α-Helix, 7.3% for β-Sheet, 14.9% for β-Turn, 22.1% for random coil. Independent-samples T tests showed that US did not significantly change the secondary structure of DLvP ($p > 0.05$). These results were consistent with the literature reporting that cavitation shearing might disrupt tertiary structure but allow most of the secondary structure intact [48,49]. Hu et al. [49] reported that US did

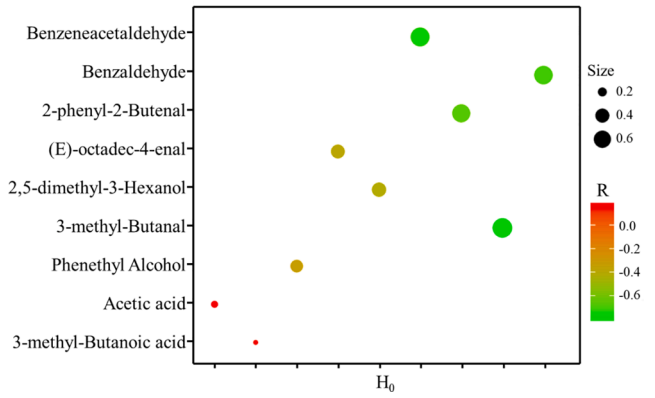

Fig. 6. A correlation plot of H0 and metabolites subjected to ultrasound pretreatment. Each circle indicates the Pearson's correlation coefficient values (r).

not change the secondary structure of soybean β-conglycinin in Tris-HCl buffer. Similarly, Zhang et al. [11] noticed that the secondary structure of peanut protein isolate was not affected significantly by ultrasonic treatment.

3.5. Correlation analysis and the proposing of potential mechanisms

To evaluate the interdependence between volatile markers and H0, a correlation plot was used to determine the correlations between the levels of identified marker metabolites using Pearson's correlation testing in Fig. 6. H0 accumulation was negatively correlated with the abundance of aldehydes, including benzaldehyde, 3-methyl-butanal, benzeneacetaldehyde, (E)-octadec-4-enal, 2-phenyl-2-butenal, 2, 5-dimethyl-3-hexanol. It is worth noting that benzaldehyde, 3-methyl-butanal, benzeneacetaldehyde and 2-phenyl-2-butenal have a strong correlation with H0 ($r > 0.67$). Moreover, phenthyl alcohol was negatively correlated with H0. However, the acids were positively correlated with H0, including acetic acid and 3-methyl-butanoic acid.

The secondary structure of DLvP remained unaffected, including α-helix, β-sheet, β-turn and random coil, when exposed to low-frequency US pretreatment. Meanwhile, the SH, S-S and molecular weight also kept unchanged. However, the surface hydrophobicity can be significantly increased ($p < 0.05$), mainly due to the change of tertiary structural caused by cavitation phenomenon. These structural features have indicated the induction of a structurally molten globule (MG)-state-like protein by US pretreatment, which comprises a series of partially structured states undergoing relatively fast conformational interchange [50]. During cavitation, micro bubbles are distributed throughout the aqueous DLvP system, and violently collapsed when the bubbles reach the maximum critical interfacial tension. The implosion of cavitation bubbles leads to energy accumulation in hot spots, thus producing high temperatures, turbulence and high pressure in local conditions [51,52]. It has been validated recently that both pressurization and heating steps can induce the formation of MG-state protein [53,54], and in turn it is reasonable to infer that the MG-state production was linked to the combined effects of pressure and heat occurring during US pretreatment.

The US-induced MG-state protein can be closely associated with the off-flavor release. As a stable monomeric intermediate, the MG-state can cause more binding sites exposed to the microenvironment with unfolding of protein, and then the less tightly packed structure of MG-state influence ligand binding by change the affinity between flavor compound to protein [54,55]. The increased binding ability of volatiles has been proven in the case of heat-induced MG-state of β-lactoglobulin [53]. Thus, the changing pattern of volatilome evolution responding to US treatments was attributed to the formation of MG-state, and the exposed hydrophobic binding sites are more favorable for the binding of volatiles (Fig. 7), thus explaining the decrease in off-flavor components of DLv samples.

4. Conclusions

This work firstly investigated the potential of ultrasound technology to reduce the off-flavor perception intensity of liver products. Results suggested that ultrasound pretreatment can inhibit the off-flavor perception by promoting the absorption of headspace aldehydes and alcohols, which was considered to be the main source of off-flavor present in livers. The structural characterization of DLvP suggested that US induced the formation of MG-state which is characterized by the increase of surface hydrophobicity and the changes of protein tertiary structure, leaving most of the secondary structural elements intact. This could be the major reason explaining the variation in the headspace concentrations of flavor compounds in terms of protein-flavor interaction and the decrease in the off-flavor perception, as confirmed by sensory evaluation and E-nose. In this regard, ultrasound can be seen a promising method that can be used independently to regulate the retention of flavor and reduce olfactory characteristics of off-flavor. However, the kinetics of US-induced MG-state protein formation under mild ultrasonic treatments and its quantitative relationship with

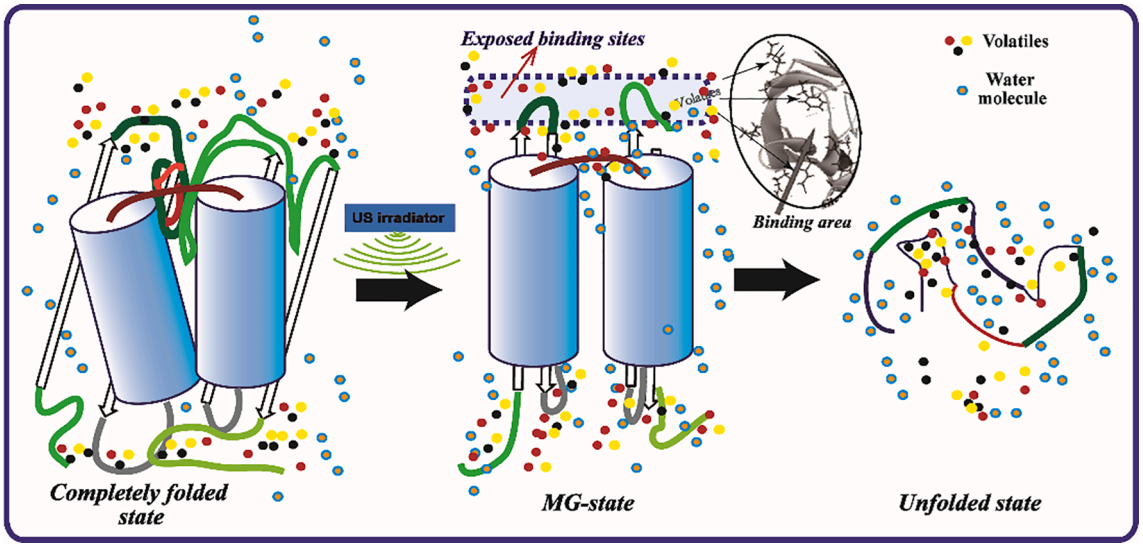

Fig. 7. The proposed mechanism for the relationship between US-induced protein modification and the volatilome evolution of DLv.

the binding behavior of flavor compounds require further research in the future work.

CRediT authorship contribution statement

Le Xu: Data curation, Investigation, Methodology, Formal analysis. **Qiang Xia:** Conceptualization, Data curation, Formal analysis, Funding acquisition, Investigation, Project administration. **Jinxuan Cao:** Data curation, Funding acquisition, Methodology, Project administration, Supervision. **Jun He:** Formal analysis, Visualization. **Changyu Zhou:** Resources, Software, Visualization. **Yuxing Guo:** Visualization, Methodology, Validation. **Daodong Pan:** Project administration, Funding acquisition, Validation, Supervision.

Declaration of Competing Interest

The authors declare that they have no known competing financial interests or personal relationships that could have appeared to influence the work reported in this paper.

Acknowledgement

This work is financially supported by the Natural Science Foundation of Zhejiang Province (LQ20C200007) and of Ningbo City (2019A610430), as well as National Natural Science Foundation of China (31871825), and Modern Agricultural Technical System Foundation (CARS-43-17).

Appendix A. Supplementary data

Supplementary data to this article can be found online at https://doi.org/10.1016/j.ultsonch.2020.105358.

References:

[1] E. Bou-Maroun, N. Cayot, Odour-active compounds of an Eisenia foetida protein powder. Identification and effect of delipidation on the odour profile, Food Chem. 124 (3) (2011) 889–894.
[2] S. Straßer, P. Schieberle, Characterization of the key aroma compounds in roasted duck liver by means of aroma extract dilution analysis: comparison with beef and pork livers, Eur Food Res Technol 238 (2) (2014) 307–313.
[3] M. Herrera-Jiménez, H. Escalona-Buendía, E. Ponce-Alquicira, R. Verde-Calvo, I. Guerrero-Legarreta, Release of Five Indicator Volatiles from a Model Meat Emulsion to Study Phase Contribution to Meat Aroma, Int. J. Food Prop. 10 (4) (2007) 807–818.
[4] J. Kühn, Thérèse Considine, H. Singh, Binding of Flavor Compounds and Whey Protein Isolate as Affected by Heat and High Pressure Treatments, J. Agric. Food Chem. 56 (21) (2008) 10218–10224.
[5] I. Suppavorasatit, K.R. Cadwallader, Effect of Enzymatic Deamidation of Soy Protein by Protein–Glutaminase on the Flavor-Binding Properties of the Protein under Aqueous Conditions, J. Agric. Food Chem. 60 (32) (2012) 7817–7823.
[6] K. Wang, S.D. Arntfield, Probing the molecular forces involved in binding of selected volatile flavour compounds to salt-extracted pea proteins, Food Chem. 211 (2016) 235–242.
[7] J. Wang, M. Zhao, C. Qiu, W. Sun, Effect of malondialdehyde modification on the binding of aroma compounds to soy protein isolates, Food Res. Int. 105 (2018) 150–158.
[8] J. Guo, Z.Y. He, S.F. Wu, M.M. Zeng, J. Chen, Effects of concentration of flavor compounds on interaction between soy protein isolate and flavor compounds, Food Hydrocolloids 100 (2020), 105388.
[9] Q. Xia, B.D. Green, Z. Zhu, Y. Li, S.M.T. Gharibzahedi, S. Roohinejad, F.J. Barba, Innovative processing techniques for altering the physicochemical properties of wholegrain brown rice (*Oryza sativa L.*) – opportunities for enhancing food quality and health attributes, Crit. Rev. Food Sci. Nutr. 59 (20) (2019) 3349–3370.
[10] L. Zhang, P. Wang, X. Sun, F. Chen, S. Lai, H. Yang, Calcium permeation property and firmness change of cherry tomatoes under ultrasound combined with calcium lactate treatment, Ultrason. Sonochem. 60 (2020) 104784, https://doi.org/10.1016/j.ultsonch.2019.104784.
[11] Q.-T. Zhang, Z.-C. Tu, H. Xiao, H. Wang, X.-Q. Huang, G.-X. Liu, C.-M. Liu, Y. Shi, L.-L. Fan, D.-R. Lin, Influence of ultrasonic treatment on the structure and emulsifying properties of peanut protein isolate, Food Bioprod. Process. 92 (1) (2014) 30–37.
[12] X. Wang, M. Majzoobi, A. Farahnaky, Ultrasound-assisted modification of functional properties and biological activity of biopolymers: A review, Ultrason. Sonochem. 65 (2020) 105057, https://doi.org/10.1016/j.ultsonch.2020.105057.
[13] Z.Y. Li, J.Y. Wang, B.D. Zheng, Z.B. Guo, Impact of combined ultrasound-microwave treatment on structural and functional properties of golden threadfin bream (*Nemipterus virgatus*) myofibrillar proteins and hydrolysates, Ultrason. Sonochem. 65 (2020), 105063.
[14] S. Petričević, N. Marušić Radovčić, K. Lukić, E. Listeš, H. Medić, Differentiation of dry-cured hams from different processing methods by means of volatile compounds, physico-chemical and sensory analysis, Meat Sci. 137 (2018) 217–227.
[15] K. Wang, S.D. Arntfield, Modification of interactions between selected volatile flavour compounds and salt-extracted pea protein isolates using chemical and enzymatic approaches, Food Hydrocolloids 61 (2016) 567–577.
[16] G. Xiong, X. Gao, P. Wang, X. Xu, G. Zhou, Comparative study of extraction efficiency and composition of protein recovered from chicken liver by acid–alkaline treatment, Process Biochem. 51 (10) (2016) 1629–1635.
[17] X. Zhang, H. Wang, X. Li, Y. Sun, D. Pan, Y. Wang, J. Cao, Effect of cinnamon essential oil on the microbiological and physiochemical characters of fresh Italian style sausage during storage, Anim Sci J 90 (3) (2019) 435–444.
[18] Q. Xia, T. Feng, X. Lou, Y. Wang, Y. Sun, D. Pan, J. Cao, Headspace fingerprinting approach to identify the major pathway influencing volatile patterns of vinasse-cured duck processed by high pressure, as well as its impact on physicochemical and sensory attributes, Int J Food Sci Technol 55 (2) (2020) 669–680.
[19] X. Lou, Q. Yang, Y. Sun, D. Pan, J. Cao, The effect of microwave on the interaction of flavour compounds with G-actin from grass carp (Catenopharyngodon idella) : Effect of microwave on flavour adsorption of G-actin, J. Sci. Food Agric 97 (12) (2017) 3917–3922.
[20] X.J. Du, Y.Y. Sun, D.D. Pan, Y. Wang, C.R. Ou, J.X. Cao, Change of the structure and the digestibility of myofibrillar proteins in Nanjing dry-cured duck during processing, J. Sci. Food Agric. 98 (2018) 3140–3147.
[21] J. Liu, Z.C. Tu, Y.H. Shan, H. Wang, G.X. Liu, X.M. Sha, L. Zhang, P. Yang, Improved antioxidant activity and glycation of alpha-lactalbumin after ultrasonic pretreatment revealed by high-resolution mass spectrometry, J. Agric. Food Chem. 65 (2017) 10317–10324.
[22] A.L. Sikes, R. Mawson, J. Stark, R. Warner, Quality properties of pre- and post-rigor beef muscle after interventions with high frequency ultrasound, Ultrason. Sonochem. 21 (6) (2014) 2138–2143.
[23] H.-J. Chang, X.-L. Xu, G.-H. Zhou, C.-B. Li, M. Huang, Effects of Characteristics Changes of Collagen on Meat Physicochemical Properties of Beef Semitendinosus Muscle during Ultrasonic Processing, Food Bioprocess Technol 5 (1) (2012) 285–297.
[24] S.D. Jayasooriya, P.J. Torley, B.R. D'Arcy, B.R. Bhandari, Effect of high power ultrasound and ageing on the physical properties of bovine Semitendinosus and Longissimus muscles, Meat Sci. 75 (4) (2007) 628–639.
[25] L. Zhang, S. Zhao, S. Lai, F. Chen, H. Yang, Combined effects of ultrasound and calcium on the chelate-soluble pectin and quality of strawberries during storage, Carbohyd. Polym. 200 (2018) 427–435.
[26] X. Chen, X. Du, J. Shen, L. Lu, W. Wang, Effect of various dietary fats on fatty acid profile in duck liver: Efficient conversion of short-chain to long-chain omega-3 fatty acids, Exp. Biol. Med. 242 (2016) 80–87.
[27] L. Rodriguez-Turienzo, A. Cobos, O. Diaz, Effects of edible coatings based on ultrasound-treated whey proteins in quality attributes of frozen Atlantic salmon (*Salmo salar*), Innovative Food Science & Emerging Technologies 14 (2012) 92–98.
[28] Y. Zou, D. Kang, R. Liu, J. Qi, G. Zhou, W. Zhang, Effects of ultrasonic assisted cooking on the chemical profiles of taste and flavor of spiced beef, Ultrason. Sonochem. 46 (2018) 36–45.
[29] Q. Wang, L.u. Li, W.u. Ding, D. Zhang, J. Wang, K. Reed, B. Zhang, Adulterant identification in mutton by electronic nose and gas chromatography-mass spectrometer, Food Control 98 (2019) 431–438.
[30] M. Estevez, S. Ventanas, R. Ramirez, R. Cava, Analysis of volatiles in porcine liver pates with added sage and rosemary essential oils by using SPME-GC-MS, J. Agric. Food Chem. 52 (2004) 5168–5174.
[31] C. Pérez-Santaescolástica, J. Carballo, E. Fulladosa, V. Garcia-Perez José, J. Benedito, J.M. Lorenzo, Application of temperature and ultrasound as corrective measures to decrease the adhesiveness in dry-cured ham. Influence on free amino acid and volatile compound profile, Food Res. Int. 114 (2018) 140–150.
[32] Y. Liu, X.-L. Xu, G.-H. Zhou, Comparative study of volatile compounds in traditional Chinese Nanjing marinated duck by different extraction techniques, Int J Food Sci Tech 42 (5) (2007) 543–550.
[33] D.L. Garcia-Gonzalez, R. Aparicio, R. Aparicio-Ruiz, Volatile and amino acid profiling of dry cured hams from different swine breeds and processing methods, Molecules 18 (2013) 3927-3947.
[34] S. Al-Dalali, F.P. Zheng, B.G. Sun, F. Chen, P. Wang, W.P. Wang, Determination of the aroma changes of Zhengrong vinegar during different processing steps by SPME-GC-MS and GC-O, J. Food Meas. Charact. 14 (2020) 535-547.
[35] J.M. Lorenzo, J. Carballo, D. Franco, Effect of the Inclusion of Chestnut in the Finishing Diet on Volatile Compounds of Dry-Cured Ham from Celta Pig Breed, Journal of Integrative Agriculture 12 (11) (2013) 2002–2012.
[36] S. IM, T. KURATA, Characterization of Off-Flavors in Porcine Liver Collected by SDE, FSTR 9 (4) (2003) 338–341.
[37] J. Zhao, M. Wang, J. Xie, M. Zhao, L.i. Hou, J. Liang, S. Wang, J. Cheng, Volatile flavor constituents in the pork broth of black-pig, Food Chem. 226 (2017) 51–60.
[38] H.M. Zhang, D. Wu, Q.L. Huang, Z.Y. Liu, X.G. Luo, S.B. Xiong, T. Yin, Adsorption kinetics and thermodynamics of yeast beta-glucan for off-odor compounds in silver carp mince, Food Chem. 319 (2020), 126232.
[39] F. Tugizimana, P.A. Steenkamp, L.A. Piater, I.A. Dubery, A conversation on data mining strategies in LC-MS untargeted metabolomics: Pre-processing and pre-treatment steps, Metabolites 6 (2016) 1–18.

[40] X. Yu, L. Chen, L. Sheng, Q. Tong, Volatile Compounds Analysis and Off-Flavors Removing of Porcupine Liver, FSTR 22 (2) (2016) 283–289.
[41] C. Arzeni, K. Martínez, P. Zema, A. Arias, O.E. Pérez, A.M.R. Pilosof, Comparative study of high intensity ultrasound effects on food proteins functionality, J. Food Eng. 108 (3) (2012) 463–472.
[42] X. Yang, Y.L. Li, S.T. Li, X.F. Ren, A.O. Oladejo, F. Lu, H.L. Ma, Effects and mechanism of ultrasound pretreatment of protein on the Maillard reaction of protein-hydrolysate from grass carp (*Ctenopharyngodon idella*), Ultrason. Sonochem. 64 (2020), 104964.
[43] H. Hu, J. Wu, E.C.Y. Li-Chan, L.e. Zhu, F. Zhang, X. Xu, G. Fan, L. Wang, X. Huang, S. Pan, Effects of ultrasound on structural and physical properties of soy protein isolate (SPI) dispersions, Food Hydrocolloids 30 (2) (2013) 647–655.
[44] H. Gao, L. Ma, T. Li, D. Sun, J. Hou, A. Li, Z. Jiang, Impact of ultrasonic power on the structure and emulsifying properties of whey protein isolate under various pH conditions, Process Biochem. 81 (2019) 113–122.
[45] I. Pallares, J. Vendrell, F.X. Aviles, S. Ventura, Amyloid fibril formation by a partially structured intermediate state of alpha-chymotrypsin, J. Mol. Biol. 342 (2004) 321–331.
[46] Y.e. Zou, H. Shi, X. Chen, P. Xu, D.i. Jiang, W. Xu, D. Wang, Modifying the structure, emulsifying and rheological properties of water-soluble protein from chicken liver by low-frequency ultrasound treatment, Int. J. Biol. Macromol. 139 (2019) 810–817.
[47] L. Jiang, J. Wang, Y. Li, Z. Wang, J. Liang, R. Wang, Y. Chen, W. Ma, B. Qi, M. Zhang, Effects of ultrasound on the structure and physical properties of black bean protein isolates, Food Res. Int. 62 (2014) 595–601.
[48] P.B. Stathopulos, G.A. Scholz, Y.-M. Hwang, J.A.O. Rumfeldt, J.R. Lepock, E. M. Meiering, Sonication of proteins causes formation of aggregates that resemble amyloid, Protein Sci. 13 (11) (2004) 3017–3027.
[49] H. Hu, I.W.Y. Cheung, S.Y. Pan, E.C.Y. Li-Chan, Effect of high intensity ultrasound on physicochemical and functional properties of aggregated soybean beta-conglycinin and glycinin, Food Hydrocolloids 45 (2015) 102–110.
[50] M. Shimizu, Y. Kajikawa, K. Kuwajima, C.M. Dobson, Y. Okamoto, Determination of the structural ensemble of the molten globule state of a protein by computer simulations, Proteins 87 (8) (2019) 635–645.
[51] C. Wen, J. Zhang, H. Zhang, C.S. Dzah, M. Zandile, Y. Duan, H. Ma, X. Luo, Advances in ultrasound assisted extraction of bioactive compounds from cash crops – A review, Ultrason. Sonochem. 48 (2018) 538–549.
[52] P.R. Gogate, A.M. Kabadi, A review of applications of cavitation in biochemical engineering/biotechnology, Biochem. Eng. J. 44 (1) (2009) 60–72.
[53] L. Tavel, C. Moreau, S. Bouhallab, E.C.Y. Li-Chan, E. Guichard, Interactions between aroma compounds and beta-lactoglobulin in the heat-induced molten globule state, Food Chem. 119 (2010) 1550–1556.
[54] J. Yang, A.K. Dunker, J.R. Powers, S. Clark, B.G. Swanson, beta-Lactoglobulin molten globule induced by high pressure, J. Agr. Food Chem. 49 (2001) 3236–3243.
[55] J. Yang, J.R. Powers, S. Clark, A.K. Dunker, B.G. Swanson, Ligand and flavor binding functional properties of beta-lactoglobulin in the molten globule state induced by high pressure, J. Food Sci. 68 (2003) 444–452.